agronomy

MDPI

Article

OsChlC1, a Novel Gene Encoding Magnesium-Chelating Enzyme, Affects the Content of Chlorophyll in Rice

Wei Lu [1], Yantong Teng [2], Fushou He [3], Xue Wang [3], Yonghua Qin [1], Gang Cheng [1], Xin Xu [1], Chuntai Wang [1] and Yanping Tan [1,*]

[1] Hubei Provincial Key Laboratory for Protection and Application of Special Plants in Wuling Area of China, College of Life Science, South-Central Minzu University, Wuhan 430074, China
[2] Biotechnology Research Institute, Chinese Academy of Agricultural Sciences, Beijing 100081, China
[3] College of Life Science, South-Central Minzu University, Wuhan 430074, China
* Correspondence: yanptan@mail.scuec.edu.cn

Abstract: Leaf-color mutants in rice (*Oryza sativa* L.) are excellent models for studying chlorophyll biosynthesis and chloroplast development. In this study, a yellow-green-leaf mutant generated by ^{60}Co irradiation, *ygl9311*, was isolated: it displayed a yellow-green leaf phenotype during the complete growth cycle. Compared with the wild type, the photosynthetic pigment contents of leaves in *ygl9311* were significantly reduced, and chloroplast development was retarded. Genetic analysis indicated that the *ygl9311* phenotype was controlled by a single recessive nuclear gene. Map-based cloning and transcriptome sequencing analysis suggested that the candidate gene was *OsChlC1* (*BGIOSGA012976*), which encodes a Mg-chelatase I subunit. The results of CRISPR/Cas9 system and RNAi knockout tests show that mutation of *OsChlC1* could reproduce the phenotype of yellow-green leaves of the mutant *ygl9311*. In conclusion, the novel rice leaf-color gene *OsChlC1* affects the content of chlorophyll in rice, showing a relatively conserved function in *indica* and *japonica* rice cultivars.

Keywords: rice; leaf-color mutants; chlorophyll; *ygl9311*; *OsChlC1*; Mg-chelatase; OsChlI subunit

check for updates

Citation: Lu, W.; Teng, Y.; He, F.; Wang, X.; Qin, Y.; Cheng, G.; Xu, X.; Wang, C.; Tan, Y. *OsChlC1*, a Novel Gene Encoding Magnesium-Chelating Enzyme, Affects the Content of Chlorophyll in Rice. *Agronomy* **2023**, *13*, 129. https://doi.org/10.3390/agronomy13010129

Academic Editor: Guodong Lu

Received: 24 November 2022
Revised: 27 December 2022
Accepted: 28 December 2022
Published: 30 December 2022

Copyright: © 2022 by the authors. Licensee MDPI, Basel, Switzerland. This article is an open access article distributed under the terms and conditions of the Creative Commons Attribution (CC BY) license (https://creativecommons.org/licenses/by/4.0/).

1. Introduction

Leaf-color mutants are often generated due to disorders in chlorophyll (Chl) metabolism during plant development [1–3]. The molecular mechanism of leaf-color mutant generation remains unclear because Chl metabolism involves complex biochemical reactions [4]. Rice (*Oryza sativa* L.) is an important food crop and also one of the most widely studied model plants. For this reason, many scholars have studied rice leaf-color mutants.

So far, hundreds of rice leaf-color mutants have been identified, and more than 30 leaf-color mutant genes have been cloned [5,6]. These genes are involved mostly in the metabolic pathway of photosynthetic pigments and can be assigned into three categories. The first category refers to genes that are directly involved in the synthesis of photosynthetic pigments and whose mutation hinders this synthesis. For instance, *OsCHLH* is a gene encoding the H subunit of magnesium ion (Mg^{2+}) chelatase during Chl synthesis, and its complete knockout kills mutants [7]. *OsCAO* encodes Chl oxygenase, and its mutation leads to the delayed development of rice plants and grayish-green leaves [8]. *YGL1* encodes Chl synthase, and its mutation makes rice leaves yellow-green in the seedling stage but normal green in the grain-filling stage [9]. *OsDVR*, a gene encoding α-8-vinyl reductase, catalyzes the reduction of divinyl Chl to vinyl Chl [10]. *YGL22* encodes a chloroplast protein, and its knockout results in the yellow-green leaf phenotype in the seedling stage [11]. The second category comprises genes involved mainly in the degradation of Chl and whose mutation makes rice leaves keep the evergreen phenotype. For example, *SGR* mutations hinder the degradation of Chl and pigment-related proteins in rice [12]. *NYC1* encodes Chl *b* reductase, and its mutation represses the degradation of chloroplast grana allowing rice leaves to remain green at harvest time [13,14]. *NYC3* mediates the degradation of the

light-harvesting chromoprotein composites [15]. *NYC4* also participates in the degradation of Chl-protein composites. The third category represents genes that are involved mainly in the synthesis of photosynthetic pigments other than Chl [16]. For instance, OsPDS and β-OsLCY are key enzymes for the synthesis of carotenoid precursors [17].

Chl synthesis comprises two parts: biosynthesis of protoporphyrin IX from L-glutamyl-tRNA and then synthesis of Chl *a* and Chl *b* from protoporphyrin IX [18–21]. Mg-chelatase is one of the key rate-limiting enzymes for the synthesis of Chl from protoporphyrin IX, chelating Mg^{2+} to protoporphyrin IX to generate magnesium protoporphyrin IX [18]. Mg-chelatase is composed of three different subunits, namely CHLI (38–46 kDa), CHLD (60–87 kDa), and CHLH (140–155 kDa) [22–24]. Mg-chelatase has been proved in in vivo and in vitro recombination experiments to play its role only when all three subunits are present [22,25]. It is speculated that Mg-chelatase works through the following mechanism: Firstly, the CHLI subunit possesses ATPase activity [26]. Then, the CHLD subunit contains a protein-binding domain able to form the CHLD/CHLI complex with the CHLI subunit [26]. Finally, with the energy from ATP hydrolysis, the CHLH subunit chelates Mg^{2+} to protoporphyrin IX [27]. However, a detailed molecular mechanism of Mg-chelatase remains to be clarified. More Mg-chelatase-related genes need to be cloned to accelerate this process.

In this study, a yellow-green leaf mutant (*ygl9311*) was identified, with leaves showing the yellow-green phenotype during the complete growth cycle. Leaves of *ygl9311* had a significantly decreased content of photosynthetic pigments in contrast with the wild type. Transmission electron microscopy (TEM) observations showed small and distorted chloroplasts in the leaves of *ygl9311*, and the grana and lamellae in chloroplasts became less abundant, with blurred granum lamellae. Moreover, the candidate gene (named *OsChlC1* in this study) of *ygl9311* was located in a 403.1 kb physical interval on chromosome 3 as determined by map-based cloning in this study. The analysis showed that *OsChlC1* encoded the subunit I of Mg-chelatase, playing a key role in the Chl synthesis in rice.

2. Materials and Methods

2.1. Plant Materials and Inherited Pattern Analysis

Previously, Teng et al. obtained a yellow-green leaf mutant (*ygl9311*) by ^{60}Co-γ-ray mutagenesis from normal green leaf *indica* cultivar 9311 [28]. Normal *indica* cultivar Gangzao was crossed with mutant *ygl9311* to obtain the F_1 generation, and the F_2 population for gene mapping was obtained by selfing the F_1 plants.

The reciprocal cross experiment between mutant *ygl9311* and the *indica* cultivar Gangzao was carried out to study the genetic pattern of the yellow leaf mutant. The reciprocal cross between the cultivar 9311 and the *indica* cultivar Gangzao was taken as control. The phenotypes of the F_1 and F_2 generations were investigated, and the trait segregation ratio in F_2 generation was calculated and analyzed by chi square test.

All rice materials were planted under natural field conditions in either Wuhan, Hubei Province, China, or Lingshui, Hainan Province, China.

2.2. Measurement of Major Agronomic Traits

The mutant *ygl9311* and *indica* cultivar 9311 were planted to measure the major agronomic traits. After maturation, plant height, number of effective tillers, number of productive panicles per plant, and number of spikelets per panicle were recorded. Data of the mutant *ygl9311* and cultivar 9311 were analyzed in Microsoft Excel, and significance of difference between them was assessed using the *t*-test.

2.3. Quantitative Analysis of Chlorophyll Content

For pigment extraction, fresh leaves (second from the top) from three biological replicates were taken in the three-leaf stage, middle of tillering stage, and flowering stage. An amount of 0.15 g of fresh leaf per sample was homogenized and centrifuged in ice-cold 80% *v/v* acetone. The concentrations of chlorophyll *a* and *b* and carotenoids were calculated

by measuring the absorbance of the supernatant at wavelengths 663 nm, 645 nm, and 470 nm, respectively, using the equation of Lichtenthaler [29]. All procedures were carried out under dim green light to avoid the degradation of photosynthetic pigments.

2.4. Observations of Chloroplast Structure

Leaf samples of the mutant *ygl9311* and *indica* cultivar 9311 were harvested from the second leaf from the top of seedlings in the 1-core 2-leaf stage. The samples were fixed with 0.1 mol/L phosphate buffer (pH 7.2) containing 3% *w/v* glutaraldehyde for 4 h. They were post-fixed with 1% *v/v* osmium acid (pH 7.2) for 4 h. The samples were dehydrated with 30%, 50%, 70%, 80%, 90%, and 100% acetone and then embedded in epoxy resin SPURR. The samples were cut into approximately 1 µm thick sections with a freezing microtome. After staining, the ultrathin sections were observed under a transmission electron microscope (H-600IV, Hitachi, Tokyo, Japan).

2.5. Measurement of Total SOD Activity

Total superoxide dismutase (SOD) activity of the mutant *ygl9311* and *indica* cultivar 9311 was measured with an SOD enzyme activity assay kit from Nanjing Jiancheng Company. The kit used the xanthine oxidase method to determine the activity of SOD. Five biological replicates, each containing 0.1 g of fresh leaves from a mature plant, were analyzed.

2.6. Initial Mapping of the Mutant ygl9311 Locus with Genome Re-Sequence

Mixed-genome DNA pools of mutant *ygl9311* and *indica* cultivar 9311 were built, consisting of 100 individual genome DNA. Re-sequence of the two pools was carried out on an Illumina Hiseq2000. The re-sequence data were aligned with the *japonica* reference genomic sequence (EnsemblPlants, http://plants.ensembl.org/Oryza_sativa/Info/Index, accessed on 21 May 2018) to remove low-quality data. Softs of GATK and annovar were used to align and annotate SNPs and small indels. Then, initial mapping was conducted by screening homozygous mutation sites where the mutant *ygl9311* was not consistent with *indica* cultivar 9311.

2.7. Fine Mapping of the Mutant ygl9311 Locus and Prediction of Candidate Genes

A total of 1325 recessive F_2 plants derived from more than 5300 plants of (the mutant *ygl9311*/*indica* cultivar Gangzao) F_2 population were selected for fine mapping. According to the result of the initial mapping, seven simple sequence repeat (SSR) markers (Table 1) located on chromosome 3 were used for making the linkage map for *ygl9311* locus. Marker information was provided from a web server, Gramene (http://www.gramene.org/bd/markers/, accessed on 5 June 2018). Transcriptome data between mutant *ygl9311* and *indica* cultivar 9311 were used to predict candidate genes. Those genes located within the mapping interval and expressed differentially were considered as candidate genes. The function of candidate genes was predicted with EnsemblPlants.

Table 1. Primer sequences of SSR markers used in the mapping of *ygl9311* locus.

SSR Markers	Forward Primer (5′-3′)	Reverse Primer (5′-3′)
RM15177	TCCTGTGTTGGACGGAGTATGC	GCCTCAGAGGTTAGAAGACAGACAGC
RM15189	GGTATCTCCCAGACACACATAGTGG	GATTGTCTCCATATCTCAGCATCC
RM15217	AAGAACCCACCTGCGGTTAGC	CTACAGCTTTCTTGATTCGCTTGG
RM15245	AGGATTTACACGCGCTTTGAGC	CATCAACGGCAGTAGAAGGTTTCC
RM15303	GAATCGGGTCTACGGTTTAGG	AAAGGAAGAGAAGAGGCAACG
RM15313	GATAAGGACATGGTGTGGTCACG	GGCCAACTAAGCACAACAAATACC
RM15355	GTAGGAAATTCTTCGCCAGATGC	CCGAGACTTGGAACAATCTTAGGC

2.8. Validation of the Function of Candidate Gene

To validate the function of candidate gene (*OsChlC1*), the knockout construct of *OsChlC1* was built through the gene-editing vector CRISPR/Cas9 [30]. Two specific editing fragments

were amplified with the primers F1 5′-GGCAGCACCGTGTCGAGCGCGTA-3′ and 5′-AAACTACGCGCTCGACACGGTGC-3′ and F2 5′-GGCAGCCGCCGTGTACCCTTCTA-3′ and 5′-AAACTAGAAGGGTACACGGCGGC-3′. The two specific editing sites were then inserted into the entry vector SK-gRNA. The gRNA-F1 and gRNA-F2 fragments were cloned into the binary vector pCAMBIA1300-Cas9. The resulting construct was designated as pCAMBIA1300-*Cas9-OsChlC1* and was transformed into japonica cultivar Nipponbare by *Agrobacterium*-mediated transformation. Primers 5′-GAATCCCTCAGCATTGTTC-3′ and 5′-TTGCGTCGTGCAGTCTGT-3′ were designed to detect the editing sites in the positive transgenic plants.

The RNAi construct of *OsChlC1* was also built in the vector DS1301. The specific interference fragment was amplified with the primers 5′-TAAACTAGTGGTACCGAACGCCTTGACACCATCGG-3′ and 5′-TAAGAGCTCGGATCCAATCCCTTCGAGACTTGGGTG-3′. The forward primer contained a *Kpn*I and an *Spe*I site, and the reverse primer contained an *Sac*I and a *BamH*I site. The resulting construct was designated as pDS1301-*OsChlC1*-RNAi and was transformed into *indica* cultivar 9311 by *Agrobacterium*-mediated transformation.

3. Results

3.1. Inheritance Pattern of the ygl9311 Mutant

The leaf-color mutant *ygl9311* in rice was induced by ^{60}Co-γ-ray mutagenesis from *indica* rice cultivar 9311; it had yellow-green leaves during the whole growth cycle (Figure 1). To analyze the genetic pattern of the mutant *ygl9311*, direct and reciprocal crosses with the mutant *ygl9311* and *indica* rice cultivar Gangzao as parents were conducted in this study. It was found that the leaves of both direct and reciprocal cross F_1 generations were all green (Figure 1B), but both direct and reciprocal cross F_2 generations showed trait segregation of yellow-green and normal green leaves. According to statistics, 926 seedlings with green leaves and 301 seedlings with yellow-green leaves were found in the direct cross F_2 generation, and 1087 green seedlings and 349 yellow-green seedlings were identified in the reciprocal cross F_2 generation. The segregation ratio of green leaf seedlings to yellow-green leaf seedlings in direct cross (926 green: 301 yellow-green, $x^2 = 0.144 < x^2_{0.05,1} = 3.84$) and reciprocal cross (1087 green: 349 yellow-green, $x^2 = 0.379 < x^2_{0.05,1} = 3.84$) F_2 generations is consistent with the Mendelian single-gene segregation rule of 3:1. These results indicate that the mutant *ygl9311* is a recessive inheritance controlled by a single gene.

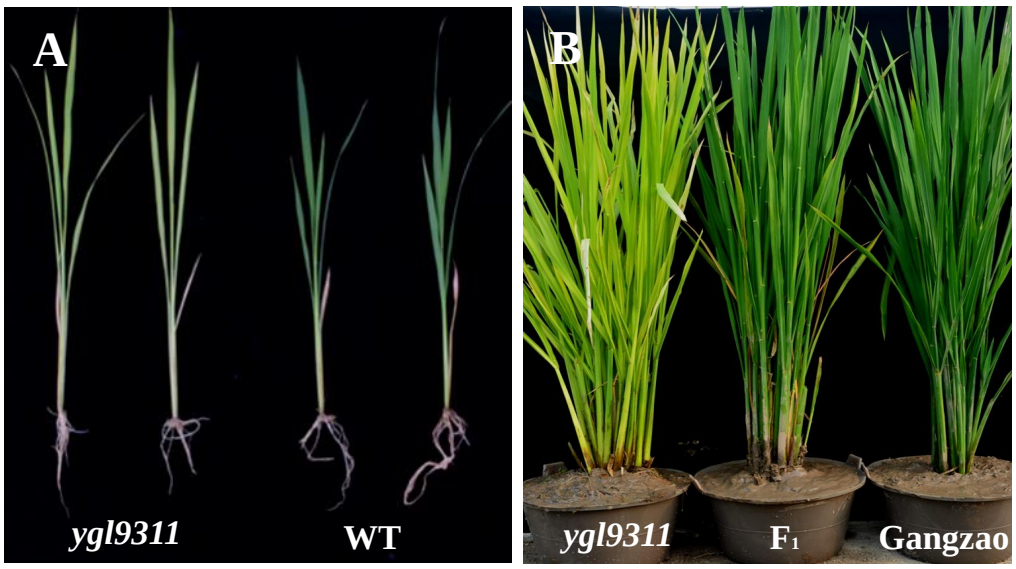


Figure 1. Phenotypic characterization of the mutant *ygl9311*. (**A**) Plants at seedling stage. (**B**) Plants at mature stage grown in Hainan.

3.2. Characteristics of the Mutant *ygl9311*

Several groups of major agronomic traits of the mutant *ygl9311* and wild *indica* cultivar 9311 were assessed in this study to explore the influence of the mutation site on the agronomic traits of rice. When planted in Wuhan, Hubei Province, China, the plant height, number of productive panicles per plant, and number of spikelets per panicle of the mutant *ygl9311* were 31.1%, 53.2%, and 20.5%, respectively, lower than those of the wild-type *indica* cultivar 9311, but the number of effective tillers per plant showed no significant difference between the mutant *ygl9311* and the *indica* cultivar 9311 (Figure 2). However, when planted in Lingshui, Hainan Province, China, the mutant *ygl9311* grew well and displayed agronomic traits, such as the plant height, comparable to the *indica* cultivar 9311. The above results signify that the mutation site affected the agronomic traits of rice plants planted in Wuhan, but they exerted less effect on agronomic traits when rice plants were planted in Hainan.

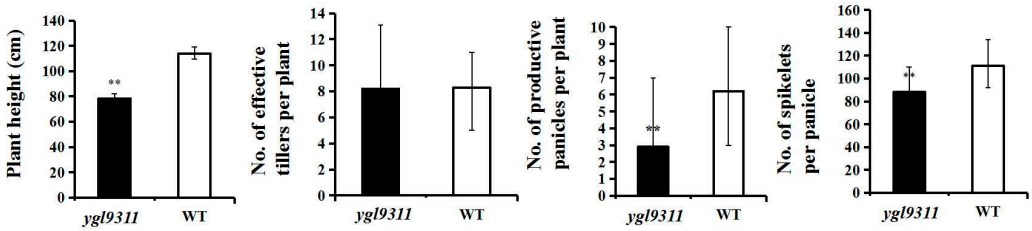


Figure 2. Comparison of major agronomic traits between mutant *ygl9311* and the wild-type parent 9311. Bars represent standard deviations of ten independent measurements. Significant differences were determined by Duncan's Multiple Range test.

The total superoxide dismutase (SOD) activity in the mutant *ygl9311* was detected to assess the effects of the mutation site on the stress resistance and antioxidant capacity of rice. The results indicate that the total SOD activity of mutant plants was 1474 U/g, slightly higher than that of the wild type (Figure 3), implying that the mutation site did not weaken the stress resistance and antioxidant capacity of rice plants.

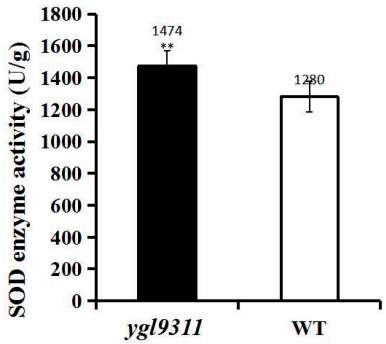


Figure 3. SOD enzyme activity in mutant *ygl9311* and the wild-type parent 9311. Bars represent standard deviations of three independent measurements. Significant differences were determined by Duncan's Multiple Range test.

Additionally, the photosynthetic pigment content in the leaves of the mutant *ygl9311* and *indica* cultivar 9311 was measured in this study at the one-core three-leaf stage, middle tillering stage, and heading stage, to investigate the physiological causes of the mutant *ygl9311*. At the above three stages, the content of Chl *a* in the mutant was, respectively, 58%, 80%, and 83% lower than that in the *indica* cultivar 9311, that of Chl *b* in the mutant was, respectively, 86%, 96%, and 99% lower than that in the *indica* cultivar 9311, and the carotenoid content in the mutant was, respectively, 58%, 77%, and 79% lower than that in the *indica* cultivar 9311 (Figure 4). The content of photosynthetic pigments was significantly lower in the mutant than in the *indica* cultivar 9311 in both the seedling stage and at

maturity, consistent with the mutant keeping yellow-green leaves during the whole growth cycle. The above results demonstrate that the change in the leaf color of the mutant is attributed mainly to decreased pigment content in mutant plants.

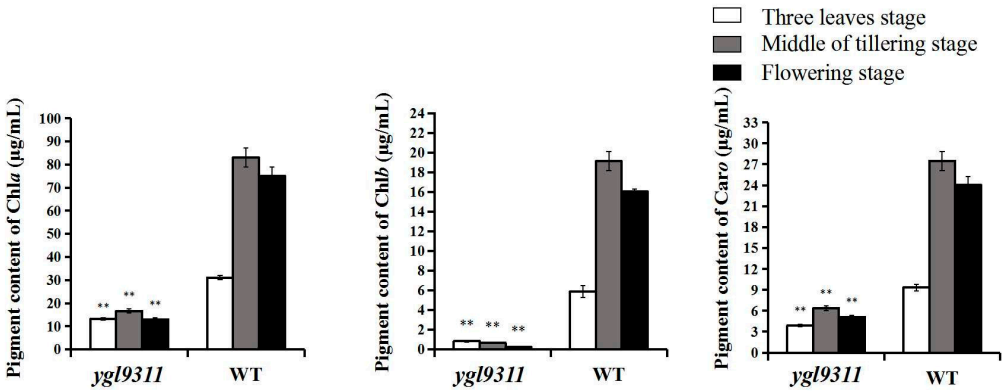


Figure 4. Photosynthetic pigment contents in leaves of the mutant *ygl9311* and the wild-type parent 9311. Bars represent standard deviations of three independent experiments. Significant differences were determined by Duncan's Multiple Range test.

To analyze further the effect of the mutation site on chloroplast development, the structure and morphology of chloroplasts in the mutant *ygl9311* and *indica* cultivar 9311 were examined by TEM (Figure 5). The results reveal that chloroplasts in the leaves of the mutant had a small size, distorted shape, and abnormal structure, in which the abundance of grana and lamellae declined, with blurred granum lamellae, fewer cristae, and obviously more osmiophilic granules. These results indicate that the mutant *ygl9311* has abnormal chloroplast development.

3.3. Map-Based Cloning of Locus of the Mutant ygl9311

In the present study, homozygous mutation sites between the mutant and the wild cultivar genome were screened out using the genome re-sequencing method to locate the mutation site of mutant *ygl9311*. According to re-sequencing results, 114,186,956 and 113,101,763 high-quality sequences with a reading length of over 100 bp were obtained in the mutant mixed pool and *indica* cultivar 9311 mixed pool, respectively. Next, the above sequences were processed with GATA software, and 4,820,964 single-nucleotide polymorphism (SNP) sites and 136,678 small InDel sites were identified. Importantly, homozygous mutation sites in the genome of the mutant were located on rice chromosomes. It was discovered that there was a SNP peak (at 20,546–21,231 Kb) on chromosome 3 (Figure 6). Therefore, it was speculated that the mutation site was located in the physical interval (20,546–21,231 Kb) on chromosome 3.

Thereafter, a F_2 population was constructed with the mutant *ygl9311* and *indica* cultivar Gangzao as parents to verify the above location results and obtain the fine-mapping of the mutant site. In brief, 1325 homozygous and recessive F_2 yellow-green leaf plants were screened using SSR primers within the initial mapping interval and in both flanking regions, on chromosome 3. The results show that the mutation site was located in the genetic interval of 7.77 cM on chromosome 3 based on seven SSR markers (Figure 7A). The *ygl9311* locus was finally narrowed to two SSR markers RM15303 and RM15313. We analyzed the sequences of these two SSR markers on the EnsemblPlants database and found that the mutation site was located at the physical interval (22,403,557–22,833,663 bp) on chromosome 3, between RM15303 (366.5 kb) and RM15313 (62.2 kb), in the genome of *indica* cultivar 9311. This physical interval has a length of 430.1 kb, covering 27 encoding genes (Figure 7B).

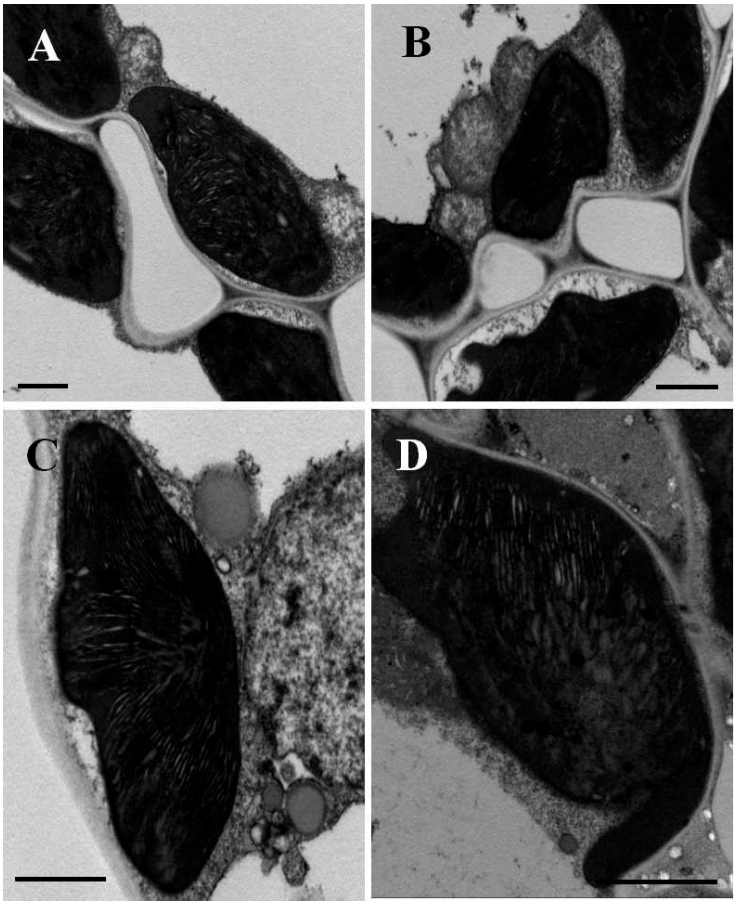


Figure 5. Electron microscope images of the mutant *ygl9311* and the wild-type plant at seedling stage. (**A**,**B**) Mesophyll cells of the wild type and *ygl9311*, respectively. (**C**,**D**) Chloroplasts of the wild type and *ygl9311*, respectively. Scale bar equals 1 μm.

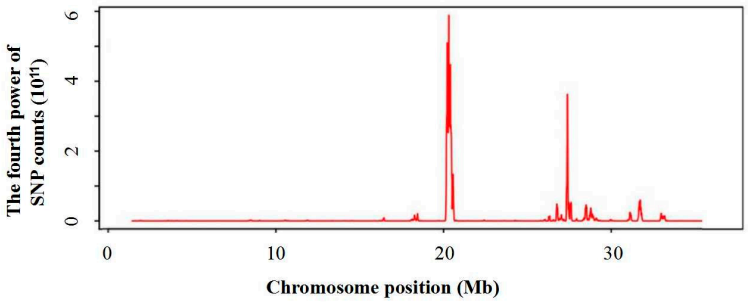


Figure 6. Distribution of SNP loci on chromosome 3. Peak at the position of 20,546–21,231 Kb on the chromosome 3 of *indica* cultivar 9311.

Transcriptome sequencing was performed between the mutant *ygl9311* and the *indica* cultivar 9311 in this study to determine the candidate gene of the mutation site. It was found that there were 217 differentially expressed genes (data not shown) between the mutant *ygl9311* and the *indica* cultivar 9311. Among these differentially expressed genes, two genes were in the physical interval of the yellow-green leaf mutation site (Table S1). Bioinformatics analysis manifested that among these differentially expressed genes, both *BGIOSGA012976* and *BGIOSGA010427* were encoding the Mg-chelatase I subunit and were implicated in chlorophyll content. However, only *BGIOSGA012976* showed sequence differences between *indica* cultivar 9311 and the mutant *ygl9311*. Therefore, it was considered in the present study that *BGIOSGA012976* was the candidate gene of the mutation *ygl9311*, and we named it *OsChlC1*.

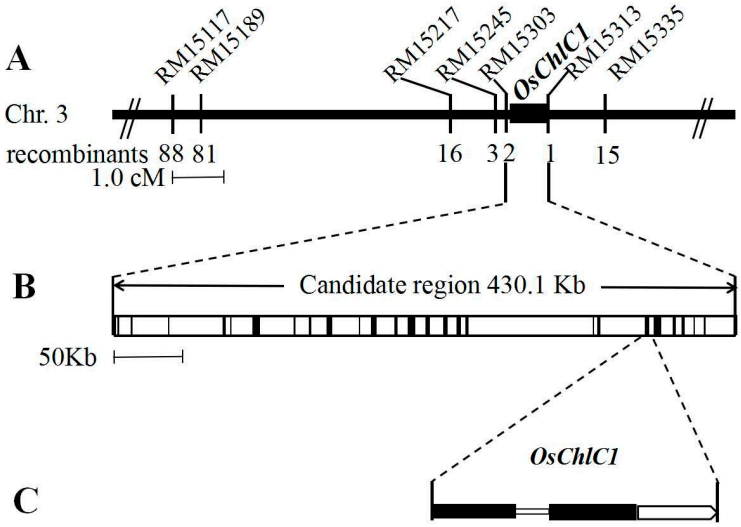


Figure 7. Molecular mapping of the *ygl9311* locus. (**A**) *OsChlC1* was narrowed between SSR markers RM15303 and RM15313 basing on analysis of 1325 recessive F_2 plants. (**B**) Total of 2 differentially expressed genes were found in the region between RM15303 and RM15313. (**C**) Candidate gene *OsChlC1* comprises two exons and one intron.

OsChlC1 is composed of two exons and one intron and has an open reading frame of 1152 bp, which can encode a polypeptide molecule consisting of 383 aa residues. In the present study, it was predicted that this gene has a chloroplast signal peptide (http://www.cbs.dtu.dk/services/TargetP/, accessed on 23 September 2020; Figure S1) at its N-terminus. According to sequence analysis, *OsChlC1* has a deletion mutation, and the first 640 bases of CDS of *OsChlC1* are absent in the genome of mutant *ygl9311*.

3.4. Validating the Function of OsChlC1

To validate the function of the candidate gene (*OsChlC1*), the knockout vector PC1300-*CAS9-OsChlC1* was constructed with the CRISPR-Cas9 technology, and genetic transformation was carried out on the *indica* cultivar 9311 with normal leaf color. Next, phenotypic identification was conducted on five transgenic rice plants that had *OsChlC1* successfully knocked out. It was uncovered that the leaf color of these rice plants with *OsChlC1* knocked out was yellow-green, consistent with that of the mutant *ygl9311* (Figure 8). Therefore, it was confirmed that the phenotype of yellow-green leaves of the mutant *ygl9311* was due to the mutation of the *OsChlC1* gene.

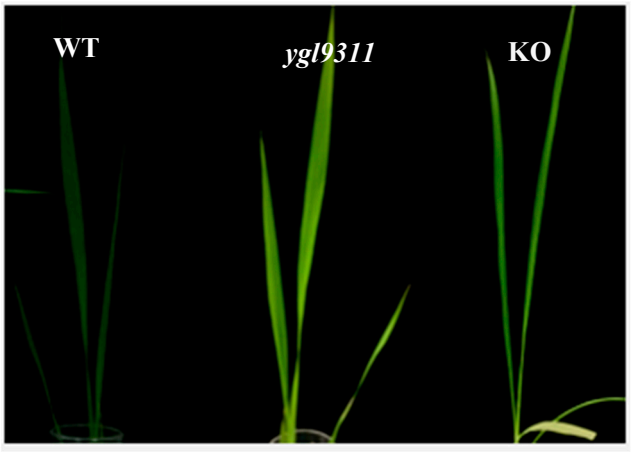


Figure 8. The phenotypes of the transgenic receptor parent *indica* 9311 (WT), mutant *ygl9311*, and knockout transgenic plant (KO) at seedling stage.

4. Discussion

In this study, the *indica* cultivar 9311 was subjected to mutation with ^{60}Co-γ-rays, and the mutant *ygl9311* with yellow-green leaves was then screened out. Next, the leaf-color gene was located by the map-based cloning strategy, cloned, and named *OsChlC1*. The results of knockout tests show that the mutant of *OsChlC1* could reproduce the phenotype of yellow-green leaves of the mutant *ygl9311*. Therefore, a new rice leaf-color gene *OsChlC1* was cloned in this study.

4.1. Chlorina Phenotype of Mutant ygl9311 Results from the Impaired Photosynthetic Pigment Synthesis

The contents of Chl *a*, Chl *b*, and carotene were significantly lower in the leaves of the mutant *ygl9311* than the *indica* cultivar 9311 in the seedling, tillering, and heading stages (Figure 4). Such a change in photosynthetic pigment content is consistent with the fact that the mutant has the traits of yellow-green leaves during the whole growth cycle. Under the catalysis of chlorophyllin a oxidase, chlorophyllin is converted into Chl *b*. The ratio Chl *a*/Chl *b* was significantly higher in the mutant *ygl9311* than the *indica* cultivar 9311 (Table S2), indicating an effect on the conversion of Chl *a* to Chl *b*. However, the ratio of total Chl content to carotene content exhibited no obvious difference between the two genotypes.

Photosynthesis-enabling protein complexes are embedded in the thylakoid membrane of chloroplasts [31–33]. The ultrastructural observation of chloroplasts revealed that the chloroplasts of the mutant *ygl9311* became smaller in size and distorted in shape, with an obviously decreased number of grana and lamellae (Figure 5). The above results indicate that the decrease in photosynthetic pigment content in the mutant *ygl9311* is the key factor leading to the phenotype of yellow-green leaves during the whole growth cycle. Moreover, the decrease in photosynthetic pigment content in the mutant *ygl9311* was associated with the defective development of chloroplasts.

4.2. The Mutation of OsChlC1 Results in Decreased Photosynthetic Pigment Content in ygl9311

Using a F_2 mapping population, the mutant gene was localized on chromosome 3, and its candidate gene *BGIOSGA012976* was cloned. The results of function prediction revealed that the gene encoded the Mg-chelatase I subunit; hence, the gene was named *OsChlC1*. The CRISPR-Cas9 technique was employed to create a mutant of the *indica* cultivar 9311 with *OsChlC1* knocked out. These transgenic *indica* rice plants showed the same yellow-green leaf phenotype as that of the yellow-leaf mutant (Figure 8). In addition, the knockout vector was transformed into the japonica rice cultivar Nipponbare, and these transgenic *japonica* rice plants also had the yellow-green leaf phenotype as that of the mutant *ygl9311* (Figure S2). The results of these two knockout experiments suggest a conserved function of *OsChlC1* in *indica* and *japonica* rice cultivars. Moreover, the knockout tests in both *indica* and *japonica* rice cultivars fully proved that *OsChlC1* mutation gives rise to the phenotype of yellow-green leaves.

4.3. OsChlC1 Is a Novel Mg-Chelatase Gene

As one of the key rate-limiting enzymes in chloroplast synthesis, Mg-chelatase binds Mg^{2+} to protoporphyrin IX to generate magnesium protoporphyrin IX [34,35]. Mg-chelatase is a complex protein composed of I, D, and H subunits [36]. Subunit I is a member of the AAA+ superfamily and has ATPase activity, whereas subunit D can form a binary complex with subunit I and interact with subunit H to insert Mg into protoporphyrin IX [37]. The Chl I subunit, an AAA+ ATPase, is responsible for the hydrolysis of ATP [38], with two very conserved domains, walker A and walker B, at its N-terminus, with walker A binding stably to ATP and walker B promoting the hydrolysis of ATP [39,40].

Many *CHLI* genes have been cloned in green plants. Two *CHLI* genes, namely *CHLI1* and *CHLI2*, exist in *Arabidopsis*. *AtCHLI1* mutation leads to the phenotype of gray-green leaves [41]. In rice, a point mutation on the third exon in the *OsCHLI* gene in the *Chlorina-9*

mutant weakens the Mg-chelatase activity [42]. A follow-up study showed that in the *Chlorina-9* mutant, the CHLI subunit could not bind to the CHLD subunit to trigger the synthesis of Mg protoporphyrin IX. *OsCHLI* comprises three exons and two introns and encodes 415 Aa residues. The *Chlorina-9* mutant of rice has the phenotype of yellow-green leaves at the three-leaf stage, but its leaf color returns to normal green in the heading stage [42]. In the present study, *OsChlC1*, a new Mg-chelatase I subunit gene, was cloned in the mutant *ygl9311*. *OsChlC1* encoded 383 aa residues and was composed of exons and one intron. The mutant *ygl9311* exhibited the phenotype of yellow-green leaves during the whole growth cycle of rice. In conclusion, *OsChlC1* is a newly cloned Mg-chelatase I subunit gene in rice, and its mutation reduces the content of chlorophyll in rice, leading to the phenotype of yellow-green leaves.

Although a series of results were obtained in this study, there are still some studies to be further improved. We constructed the ectopic expression vector of the *OsChlC1* gene, and genetic transformation is already in progress. However, no positive plants have been obtained from the complementary assay. On the other hand, CRISPR/Cas9 system and RNAi knockout tests showed that the mutant of *OsChlC1* could reproduce the phenotype of yellow-green leaves of the mutant *ygl9311*, but we still need to determine the content of chlorophyll in the above mutant leaves. Gene function prediction indicates that *OsChlC1* encodes Mg-chelatase subunit I. In order to verify the function of *OsChlC1*, we need to detect the activity of magnesium ion chelatase in different mutants.

5. Conclusions

In this study, the candidate gene *OsChlC1* of the rice yellow-green leaf mutant *ygl9311* was cloned. According to the sequence analysis and function prediction, *OsChlC1* encoding 383 aa residues is a new Mg-chelatase I subunit gene. In addition, *OsChlC1* knockout in the *indica* rice cultivar 9311 and the *japonica* rice cultivar Nipponbare had the phenotype of yellow-green leaves of the mutant *ygl9311*. Therefore, we conclude that *OsChlC1* mutation in the genome of the *indica* rice cultivar 9311 leads to a decrease in chlorophyll content in rice leaves, affects chloroplast development, and results in the phenotype of yellow-green leaves of the mutant *ygl9311*. The *OsChlC1* exerts a relatively conserved function in *indica* and *japonica* rice cultivars.

Supplementary Materials: The following supporting information can be downloaded at https://www.mdpi.com/article/10.3390/agronomy13010129/s1, Figure S1: Chloroplast Signal Peptide Prediction of *OsChlC1* Gene, Figure S2: The Phenotypes of the wild-type parent 9311 (WT), mutant *ygl9311*, knockout transgenic plant (KO), and transgenic recipient parent Nipponbare (NIP) at seedling stage, Table S1: Differentially expressed genes within the physical location of the *ygl9311* mutation site, Table S2: Pigment content and ratio at various stages between *ygl9311* and wild type.

Author Contributions: Conceptualization, W.L., Y.T. (Yantong Teng) and F.H.; Data curation, W.L.; Investigation, G.C.; Methodology, W.L., Y.T. (Yantong Teng) and X.W.; Resources, C.W.; Software, Y.T. (Yantong Teng); Supervision, Y.T. (Yanping Tan); Validation, W.L., Y.Q. and X.X.; Writing—original draft, W.L.; Writing—review and editing, W.L. and Y.T. (Yanping Tan). All authors have read and agreed to the published version of the manuscript.

Funding: This research received no external funding.

Data Availability Statement: The datasets generated during the current study are available from the corresponding author on reasonable request.

Acknowledgments: The authors extend their appreciation for the support from the Hubei Provincial Key Laboratory for Protection and Application of Special Plants in Wuling Area of China, College of Life Science, South-Central Minzu University.

Conflicts of Interest: The authors declare no conflict of interest.

References

1. Khan, A.; Jalil, S.; Cao, H.; Tsago, Y.; Sunusi, M.; Chen, Z.; Shi, C.; Jin, X. The Purple Leaf (*pl6*) Mutation Regulates Leaf Color by Altering the Anthocyanin and Chlorophyll Contents in Rice. *Plants* **2020**, *9*, 1477. [CrossRef]
2. Wang, Y.; Wang, J.; Chen, L.; Meng, X.; Zhen, X.; Liang, Y.; Han, Y.; Li, H.; Zhang, B. Identification and function analysis of yellow-leaf mutant (*YX-yl*) of broomcorn millet. *BMC Plant Biol.* **2022**, *22*, 463. [CrossRef]
3. Chen, T.; Huang, L.; Wang, M.; Huang, Y.; Zeng, R.; Wang, X.; Wang, L.; Wan, S.; Zhang, L. Ethyl Methyl Sulfonate-Induced Mutagenesis and Its Effects on Peanut Agronomic, Yield and Quality Traits. *Agronomy* **2020**, *10*, 655. [CrossRef]
4. Yan, J.; Sun, P.; Liu, W.; Xie, D.; Wang, M.; Peng, Q.; Sun, Q.; Jiang, B. Metabolomic and Transcriptomic Analyses Reveal Association of Mature Fruit Pericarp Color Variation with Chlorophyll and Flavonoid Biosynthesis in Wax Gourd (*Benincasa hispida*). *Agronomy* **2022**, *12*, 2045. [CrossRef]
5. Deng, X.-J.; Zhang, H.-Q.; Wang, Y.; He, F.; Liu, J.-L.; Xiao, X.; Shu, Z.-F.; Li, W.; Wang, G.-H.; Wang, G.-L. Mapped clone and functional analysis of leaf-color gene *Ygl7* in a rice hybrid (*Oryza sativa* L. ssp. indica). *PLoS ONE* **2014**, *9*, e99564. [CrossRef]
6. Wan, C.; Li, C.; Ma, X.; Wang, Y.; Sun, C.; Huang, R.; Zhong, P.; Gao, Z.; Chen, D.; Xu, Z.; et al. *GRY79* encoding a putative metallo-β-lactamase-trihelix chimera is involved in chloroplast development at early seedling stage of rice. *Plant Cell Rep.* **2015**, *34*, 1353–1363. [CrossRef]
7. Jung, K.-H.; Hur, J.; Ryu, C.-H.; Choi, Y.; Chung, Y.-Y.; Miyao, A.; Hirochika, H.; An, G. Characterization of a rice chlorophyll-deficient mutant using the T-DNA gene-trap system. *Plant Cell Physiol.* **2003**, *44*, 463–472. [CrossRef]
8. Lee, S.; Kim, J.-H.; Yoo, E.-S.; Lee, C.-H.; Hirochika, H.; An, G. Differential regulation of chlorophyll a oxygenase genes in rice. *Plant Mol. Biol.* **2005**, *57*, 805–818. [CrossRef]
9. Wu, Z.; Zhang, X.; He, B.; Diao, L.; Sheng, S.; Wang, J.; Guo, X.; Su, N.; Wang, L.; Jiang, L.; et al. A chlorophyll-deficient rice mutant with impaired chlorophyllide esterification in chlorophyll biosynthesis. *Plant Physiol.* **2007**, *145*, 29–40. [CrossRef]
10. Wang, P.; Gao, J.; Wan, C.; Zhang, F.; Xu, Z.; Huang, X.; Sun, X.; Deng, X. Divinyl chlorophyll(ide) a can be converted to monovinyl chlorophyll(ide) a by a divinyl reductase in rice. *Plant Physiol.* **2010**, *153*, 994–1003. [CrossRef]
11. Zhu, Y.; Yan, P.; Dong, S.; Hu, Z.; Wang, Y.; Yang, J.; Xin, X.; Luo, X. Map-based cloning and characterization of *YGL22*, a new yellow-green leaf gene in rice (*Oryza sativa*). *Crop Sci.* **2020**, *61*, 529–538. [CrossRef]
12. Jiang, H.; Li, M.; Liang, N.; Yan, H.; Wei, Y.; Xu, X.; Liu, J.; Xu, Z.; Chen, F.; Wu, G. Molecular cloning and function analysis of the stay green gene in rice. *Plant J.* **2007**, *52*, 197–209. [CrossRef]
13. Kusaba, M.; Ito, H.; Morita, R.; Iida, S.; Sato, Y.; Fujimoto, M.; Kawasaki, S.; Tanaka, R.; Hirochika, H.; Nishimura, M.; et al. Rice NON-YELLOW COLORING1 is involved in light-harvesting complex II and grana degradation during leaf senescence. *Plant Cell* **2007**, *19*, 1362–1375. [CrossRef]
14. Sato, Y.; Morita, R.; Katsuma, S.; Nishimura, M.; Tanaka, A.; Kusaba, M. Two short-chain dehydrogenase/reductases, NON-YELLOW COLORING 1 and NYC1-LIKE, are required for chlorophyll b and light-harvesting complex II degradation during senescence in rice. *Plant J.* **2007**, *57*, 120–131. [CrossRef]
15. Morita, R.; Sato, Y.; Masuda, Y.; Nishimura, M.; Kusaba, M. Defect in *non-yellow coloring 3*, an α/β hydrolase-fold family protein, causes a stay-green phenotype during leaf senescence in rice. *Plant J.* **2009**, *59*, 940–952. [CrossRef]
16. Yamatani, H.; Sata, Y.; Masuda, Y.; Kato, Y.; Morita, R.; Fukunaga, K.; Nagamura, Y.; Nishimura, M.; Sakamoto, W.; Tanaka, A.; et al. *NYC4*, the rice ortholog of Arabidopsis *THF1*, is involved in the degradation of chlorophyll-protein complexes during leaf senescence. *Plant J.* **2013**, *74*, 652–662. [CrossRef]
17. Fang, J.; Chai, C.; Qian, Q.; Li, C.; Tang, J.; Sun, L.; Huang, Z.; Guo, X.; Sun, C.; Liu, M.; et al. Mutations of genes in synthesis of the carotenoid precursors of ABA lead to pre-harvest sprouting and photo-oxidation in rice. *Plant J.* **2008**, *54*, 177–189. [CrossRef]
18. Beale, S.I. Green genes gleaned. *Trends Plant Sci.* **2005**, *10*, 309–312. [CrossRef]
19. Bollivar, D.W. Recent advances in chlorophyll biosynthesis. *Photosynth. Res.* **2006**, *90*, 173–194. [CrossRef]
20. Qiu, N.; Jiang, D.; Wang, X.; Wang, B.; Zhou, F. Advances in the members and biosynthesis of chlorophyll family. *Photosynthetica* **2019**, *57*, 974–984. [CrossRef]
21. Zhang, H.; Liu, L.; Cai, M.; Zhu, S.; Zhao, J.; Zheng, T.; Xu, X.; Zeng, Z.; Niu, J.; Jiang, L.; et al. A point mutation of magnesium chelatase *OsCHLI* gene dampens the interaction between CHLI and CHLD subunits in rice. *Plant Mol. Biol. Rep.* **2015**, *33*, 1975–1987. [CrossRef]
22. Willows, R.D.; Gibson, L.C.; Kanangara, C.G.; Hunter, C.N.; von Wettstein, D. Three separate proteins constitute the magnesium chelatase of *Rhodobacter* sphaeroides. *Eur. J. Biochem.* **1996**, *15*, 438–443. [CrossRef]
23. Kannangara, C.G.; Vothknecht, U.C.; Hansson, M.; von Wettstein, D. Magnesium chelatase: Association with ribosomes and mutant complementation studies identify barley subunit Xantha-G as a functional counterpart of *Rhodobacter* subunit BchD. *Mol. Gen. Genet. MGG* **1997**, *18*, 85–92. [CrossRef]
24. Davison, P.A.; Schubert, H.L.; Reid, J.D.; Iorg, C.D.; Heroux, A.; Hill, C.P.; Hunter, C.N. Structural and biochemical characterization of Gun4 suggests a mechanism for its role in chlorophyll biosynthesis. *Biochemistry* **2005**, *31*, 7603–7612. [CrossRef]
25. Gibson, L.C.; Willows, R.D.; Kannangara, C.G.; von Wettstein, D.; Hunter, C.N. Magnesium-protoporphyrin chelatase of *Rhodobacter* sphaeroides: Reconstitution of activity by combining the products of the bchH, -I, and -D genes expressed in Escherichia coli. *Proc. Natl. Acad. Sci. USA* **1995**, *92*, 1941–1944. [CrossRef]
26. Sirijovski, N.; Olsson, U.; Lundqvist, J.; Al-Karadaghi, S.; Willows, R.D.; Hansson, M. ATPase activity associated with the magnesium chelatase H-subunit of the chlorophyll biosynthetic pathway is an artefact. *Biochem. J.* **2006**, *400*, 477–484. [CrossRef]

27. Gräfe, S.; Saluz, H.-P.; Grimm, B.; Hänel, F. Mg-chelatase of tobacco: The role of the subunit CHL D in the chelation step of protoporphyrin IX. *Proc. Natl. Acad. Sci. USA* **1999**, *96*, 1941–1946. [CrossRef]
28. Teng, Y.; Ye, L.; He, F.; Chu, W.; Wang, C.; Tan, Y. Expression Analysis of Key Genes of Chlorophyll Synthesis in A Yellow Leaves Mutant of Oryza sativa. *Chin. Agric. Sci. Bull.* **2017**, *33*, 30–35.
29. Lichtenthaler, H.K. [34] Chlorophylls and carotenoids: Pigments of photosynthetic biomembranes. *Methods Enzymol.* **1987**, *148*, 350–382.
30. He, F.; Shao, M.; Chen, T.; Wang, C.; Xu, X.; Tan, Y. Knockout of a magnesium chelating enzyme gene in rice using CRISPR-Cas9 system. *Fenzi Zhiwu Yuzhong (Mol. Plant Breed.)* **2019**, *17*, 5674–5680.
31. Pipitone, R.; Eicke, S.; Pfister, B.; Glauser, G.; Falconet, D.; Uwizeye, C.; Pralon, T.; Zeeman, S.C.; Kessler, F.; Demarsy, E. A multifaceted analysis reveals two distinct phases of chloroplast biogenesis during de-etiolation in *Arabidopsis*. *Elife* **2021**, *10*, e62709. [CrossRef]
32. Sandoval-Ibáñez, O.; Sharma, A.; Bykowski, M.; Borràs-Gas, G.; Behrendorff, J.B.Y.H.; Mellor, S.; Qvortrup, K.; Verdonk, J.C.; Bock, R.; Kowalewska, Ł.; et al. Curvature thylakoid 1 proteins modulate prolamellar body morphology and promote organized thylakoid biogenesis in *Arabidopsis thaliana*. *Proc. Natl. Acad. Sci. USA* **2021**, *118*, e2113934118. [CrossRef]
33. Allen, J.F.; de Paula, W.B.; Puthiyaveetil, S.; Nield, J. A structural phylogenetic map for chloroplast photosynthesis. *Trends Plant Sci.* **2011**, *16*, 645–655. [CrossRef] [PubMed]
34. Wang, Z.; Hong, X.; Hu, K.; Wang, Y.; Wang, X.; Du, S.; Li, Y.; Hu, D.; Cheng, K.; An, B.; et al. Impaired Magnesium Protoporphyrin IX Methyltransferase (ChlM) Impedes Chlorophyll Synthesis and Plant Growth in Rice. *Front Plant Sci.* **2017**, *8*, 1694. [CrossRef]
35. Sawicki, A.; Willows, R.D. *S*-adenosyl-L-methionine:magnesium-protoporphyrin IX *O*-methyltransferase from *Rhodobacter capsulatus*: Mechanistic insights and stimulation with phospholipids. *Biochem. J.* **2007**, *406*, 469–478. [CrossRef]
36. Adhikari, N.D.; Froehlich, J.E.; Strand, D.D.; Buck, S.M.; Kramer, D.M.; Larkin, R.M. GUN4-porphyrin complexes bind the ChlH/GUN5 subunit of Mg-Chelatase and promote chlorophyll biosynthesis in *Arabidopsis*. *Plant Cell* **2011**, *23*, 1449–1467. [CrossRef] [PubMed]
37. Farmer, D.A.; Brindley, A.A.; Hitchcock, A.; Jackson, P.J.; Johnson, B.; Dickman, M.J.; Hunter, C.N.; Reid, J.D.; Adams, N.B.P. The ChlD subunit links the motor and porphyrin binding subunits of magnesium chelatase. *Biochem. J.* **2019**, *476*, 1875–1887. [CrossRef] [PubMed]
38. Lundqvist, J.; Elmlund, H.; Wulff, R.P.; Berglund, L.; Elmlund, D.; Emanuelsson, C.; Hebert, H.; Willows, R.D.; Hansson, M.; Lindahl, M.; et al. ATP-induced conformational dynamics in the AAA+ motor unit of magnesium chelatase. *Structure* **2010**, *18*, 354–365. [CrossRef] [PubMed]
39. Jessop, M.; Felix, J.; Gutsche, I. AAA+ ATPases: Structural insertions under the magnifying glass. *Curr. Opin. Struct. Biol.* **2021**, *66*, 119–128. [CrossRef]
40. Miller, J.M.; Enemark, E.J. Fundamental characteristics of AAA+ protein family structure and function. *Archaea* **2016**, *2016*, 9294307. [CrossRef] [PubMed]
41. Koncz, C.; Mayerhofer, R.; Koncz-Kalman, Z.; Nawrath, C.; Reiss, B.; Redei, G.P.; Schell, J. Isolation of a gene encoding a novel chloroplast protein by T-DNA tagging in *Arabidopsis thaliana*. *EMBO J.* **1990**, *9*, 1337–1346. [CrossRef] [PubMed]
42. Zhang, H.; Li, J.; Yoo, J.H.; Yoo, S.C.; Cho, S.H.; Koh, H.J.; Seo, H.S.; Paek, N.C. Rice *Chlorina-1* and *Chlorina-9* encode ChlD and ChlI subunits of Mg-chelatase, a key enzyme for chlorophyll synthesis and chloroplast development. *Plant Mol. Biol.* **2006**, *62*, 325–337. [CrossRef] [PubMed]

Disclaimer/Publisher's Note: The statements, opinions and data contained in all publications are solely those of the individual author(s) and contributor(s) and not of MDPI and/or the editor(s). MDPI and/or the editor(s) disclaim responsibility for any injury to people or property resulting from any ideas, methods, instructions or products referred to in the content.